Docosahexaenoic acid mediates peroxisomal elongation, a prerequisite for peroxisome division

Akinori Itoyama[1], Masanori Honsho[2], Yuichi Abe[2], Ann Moser[3], Yumi Yoshida[2] and Yukio Fujiki[1,2,4,*]

[1]Graduate School of Systems Life Sciences, and [2]Department of Biology, Faculty of Sciences, Kyushu University Graduate School, 6-10-1 Hakozaki, Higashi-ku, Fukuoka 812-8581, Japan
[3]The Hugo W. Moser Research Institute, Kennedy Krieger Institute, Johns Hopkins University, Baltimore, MD 21205, USA
[4]CREST, Japan Science and Technology Agency, Chiyoda, Tokyo 102-0075, Japan
*Author for correspondence (yfujiki@kyudai.jp)

Accepted 17 November 2011
Journal of Cell Science 125, 589–602

doi: 10.1242/jcs.087452

Summary

Peroxisome division is regulated by several factors, termed fission factors, as well as the conditions of the cellular environment. Over the past decade, the idea of metabolic control of peroxisomal morphogenesis has been postulated, but remains largely undefined to date. In the current study, docosahexaenoic acid (DHA, C22:6n-3) was identified as an inducer of peroxisome division. In fibroblasts isolated from patients that carry defects in peroxisomal fatty acid β-oxidation, peroxisomes are much less abundant than normal cells. Treatment of these patient fibroblasts with DHA induced the proliferation of peroxisomes to the level seen in normal fibroblasts. DHA-induced peroxisomal proliferation was abrogated by treatment with a small inhibitory RNA (siRNA) targeting *dynamin-like protein 1* and with dynasore, an inhibitor of dynamin-like protein 1, which suggested that DHA stimulates peroxisome division. DHA augmented the hyper-oligomerization of Pex11pβ and the formation of Pex11pβ-enriched regions on elongated peroxisomes. Time-lapse imaging analysis of peroxisomal morphogenesis revealed a sequence of steps involved in peroxisome division, including elongation in one direction followed by peroxisomal fission. DHA enhanced peroxisomal division in a microtubule-independent manner. These results suggest that DHA is a crucial signal for peroxisomal elongation, a prerequisite for subsequent fission and peroxisome division.

Key words: Peroxisome morphogenesis, Elongation, Fission, Division, Fatty acid β-oxidation, Peroxin Pex11p, Dynamin-like protein 1, Fis1

Introduction

The peroxisome is a single-membrane-bounded organelle present in almost all eukaryotic cells. The importance of peroxisomal function is highlighted by the severe clinical manifestations of the human genetic disorders of peroxisomal biogenesis, namely the peroxisome biogenesis disorders (PBDs) and single peroxisomal enzyme deficiencies (SEDs). The primary defect in PBDs is impaired peroxisome biogenesis involving defects in membrane biogenesis and/or import of matrix proteins harboring type 1 or type 2 peroxisomal targeting signals (Fujiki, 2000; Gould and Valle, 2000; Subramani, 1998). In SEDs, the primary defect maps to specific proteins involved in peroxisomal metabolic pathways (Wanders and Waterham, 2006). Widely recognized SEDs include X-linked adrenoleukodystrophy (X-ALD), which is due to a defect in adrenoleukodystrophy protein (a member of the ATP-binding cassette transporter family) (Kemp et al., 2001; Mosser et al., 1993; Smith et al., 1999); deficiency of acyl-CoA oxidase 1 (AOx), which is specific for straight-chain fatty acids (Ferdinandusse et al., 2007; Poll-The et al., 1988); and deficiency of 2-enoyl-CoA hydratase/D-3-hydroxyacyl-CoA dehydrogenase, bifunctional protein (D-BP), (Ferdinandusse et al., 2006; Suzuki et al., 1997).

In the classic model of peroxisome biogenesis, growth and division, peroxisome growth occurs through the uptake of various newly synthesized proteins from the cytosol, followed by division (Lazarow and Fujiki, 1985). In mammalian cells, peroxisome abundance is strictly regulated by the peroxisomal division machinery and is kept constant under normal conditions. Peroxisome division is proposed to involve three stages: elongation, constriction and fission (Koch et al., 2003; Li and Gould, 2003; Schrader et al., 1998). Peroxisomes share several division factors with mitochondria, including dynamin-like protein 1 (DLP1), fission1 (Fis1) and mitochondrial fission factor, all three of which are key regulators of peroxisomal and mitochondrial morphogenesis (Gandre-Babbe and van der Bliek, 2008; Kobayashi et al., 2007; Koch et al., 2003; Koch et al., 2005; Li and Gould, 2003; Tanaka et al., 2006; Waterham et al., 2007). Pex11p is a peroxisome-specific division factor that is present in cells as three isoforms, Pex11pα (Abe et al., 1998; Li et al., 2002a), Pex11pβ (Abe and Fujiki, 1998; Li et al., 2002b; Schrader et al., 1998) and Pex11pγ (Li et al., 2002a; Tanaka et al., 2003). Pex11pβ is believed to play a role in the elongation step of peroxisome division (Li and Gould, 2002; Schrader et al., 1998), whereas DLP1 has been shown to play a crucial role at the fission stage (Koch et al., 2003; Li and Gould, 2003). Pex11pβ, Fis1 and DLP1 have been shown to coordinately regulate peroxisome division (Kobayashi et al., 2007). However, the detailed molecular mechanisms underlying the three steps remain obscure.

First reported in 1988, fibroblasts from patients with PBDs contain peroxisomes with aberrant morphology termed ‘membrane ghost’, which are larger in size but fewer in number compared with normal fibroblasts (Santos et al., 1988). Similarly, abnormal peroxisomes are observed in fibroblasts deficient in peroxisomal

fatty-acid β-oxidation enzymes, implying a potential correlation between peroxisomal morphogenesis and peroxisomal β-oxidation (Chang et al., 1999; Funato et al., 2006).

The present study was designed to address the issue of how dysfunctional peroxisomal β-oxidation could give rise to peroxisome dysmorphogenesis. Docosahexaenoic acid (DHA, C22:6n-3), a major product of peroxisomal β-oxidation, was identified as an inducer of peroxisomal division. The utility of DHA-mediated peroxisomal division as a model system for elucidating the molecular mechanisms underlying peroxisomal morphogenesis are discussed.

Results

Peroxisome abundance is significantly reduced in fibroblasts from patients with peroxisomal fatty acid β-oxidation deficiency

The abundance and morphology of peroxisomes in fibroblasts from patients with deficiencies in peroxisomal fatty acid β-oxidation were examined by immunostaining with an anti-Pex14p antibody. In normal fibroblasts, a typical punctate staining pattern indicative of peroxisomal structures was discernible (Fig. 1Aa). By contrast, there were far fewer Pex14p-positive structures, and the structures that were evident were larger in size in fibroblasts from a patient with Zellweger syndrome (defective in *PEX10*), which indicated impaired import of peroxisomal matrix proteins (Fig. 1Ab). These results were consistent with earlier reports (Okumoto et al., 1998a; Warren et al., 1998). Likewise, peroxisomes were less abundant in fibroblasts from patients that were deficient in *AOx* (Fig. 1Ac) and *D-BP* (Fig. 1Ad). Peroxisome abundance was quantified by counting the number of Pex14p-positive structures in at least 50 randomly selected cells. In normal control fibroblasts, the number of peroxisomes averaged 267±75 per cell (all results for peroxisome abundance refer to the number of peroxisomes per cell) (Fig. 1B). By contrast, in *AOx*- and *D-BP*-defective fibroblasts, peroxisomes numbered 67±24 and 86±29 per cell, respectively (Fig. 1B). These results indicated that dysfunctional peroxisomal fatty acid β-oxidation resulted in reduced peroxisome abundance, consistent with several earlier reports (Chang et al., 1999; Funato et al., 2006). Thus, impaired peroxisome morphogenesis in these cells was probably caused by either an accumulation or reduction in the level of fatty acids.

DHA levels are low in fibroblasts with impaired peroxisomal morphogenesis

We next investigated potential metabolites involved in the regulation of peroxisomal morphogenesis. In peroxisomal β-oxidation, AOx catalyzes straight-chain, but not branched-chain fatty acids such as pristanic acid and di- and tri-hydroxycholestanoic acid (Wanders, 2004). In fibroblasts from an X-ALD patient, β-oxidation activity of saturated very long chain fatty acids was impaired (Fig. 1C), even though peroxisomes were normal in terms of morphology and number (276±84 per cell) (Fig. 1Ae, Fig. 1B). We hypothesized that peroxisomal dysmorphogenesis was caused by an accumulation or reduction in the level of straight-chain and unsaturated fatty acids.

DHA is an essential poly-unsaturated fatty acid (PUFA) and a major product of peroxisomal β-oxidation (Ferdinandusse et al., 2001). DHA synthesis from dietary linolenic acid (C18:3n-3) is initiated in the endoplasmic reticulum and completed by

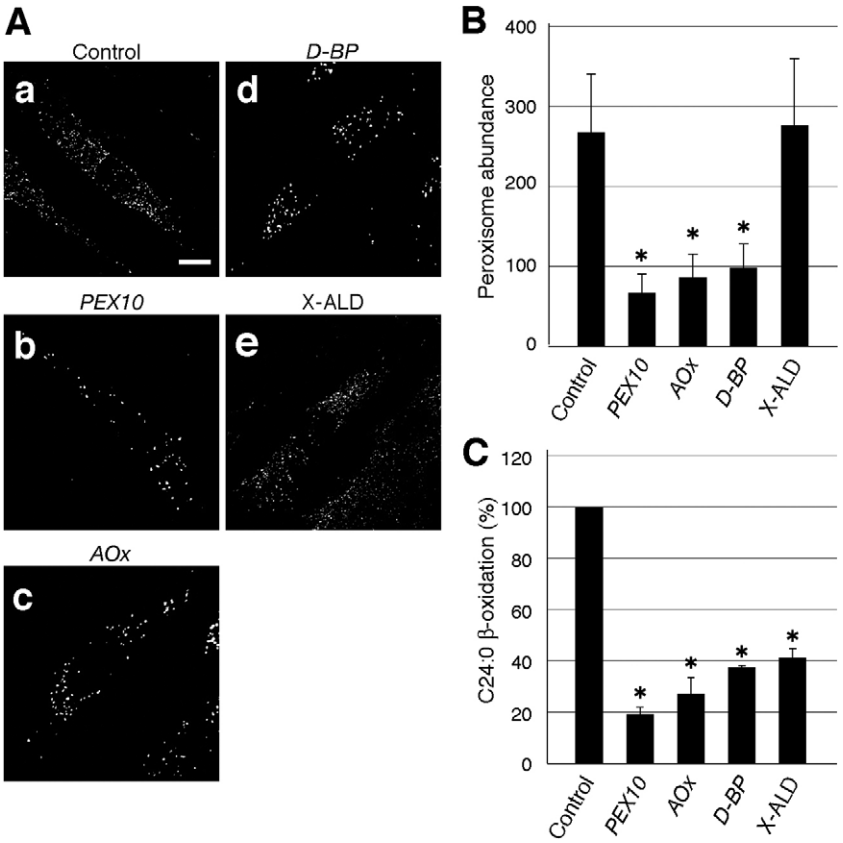

Fig. 1. Severely reduced number and aberrant morphology of peroxisomes in fibroblasts from patients with peroxisomal fatty acid β-oxidation disorders. (**A**) Fibroblasts from a normal control subject (Aa) and individual patients with deficiencies in *PEX10* (Ab), *AOx* (Ac), and *D-BP* (Ad), and an X-ALD patient (Ae) were stained with an anti-Pex14p antibody. Scale bar: 10 μm. (**B**) Peroxisome abundance per cell was determined as described in Materials and Methods. (**C**) Peroxisomal β-oxidation in control and patient-derived fibroblasts. β-oxidation in control fibroblasts was 0.76 nmol/hour/mg of protein. β-oxidation activity in the patient-derived cells was expressed relative to the control, which was set as 100%. Data represent the means ± s.d. of three independent experiments; **P*<0.01 compared with control fibroblasts.

peroxisomal β-oxidation (Ferdinandusse et al., 2001). DHA synthesis is significantly reduced in *AOx*- and *D-BP*-deficient fibroblasts, but not in fibroblasts from a patient with X-ALD (Su et al., 2001). These considerations prompted us to examine whether dysmorphogenesis of peroxisomes in fibroblasts defective in peroxisomal β-oxidation was due to a depletion of DHA.

DHA levels were determined by liquid chromatography combined with tandem mass spectrometry (LC-MS/MS). The level of DHA in *AOx*-deficient fibroblasts was approximately 50% of that in control fibroblasts, with percentages for the respective DHA-containing phospholipids ranging from 40 to 60% (Table 1). Similarly, DHA levels were reduced in fibroblasts from patients deficient in Pex10p and D-BP. By contrast, DHA levels in fibroblasts from an X-ALD patient were nearly the same as in a control cells (Table 1), consistent with an earlier report (Martinez, 1995). These results suggested that the aberrant morphology and reduced abundance of peroxisomes in fibroblasts from patients with peroxisomal β-oxidation deficiency are caused by reduced levels of DHA.

DHA restores proper peroxisome morphogenesis in *AOx*- and *D-BP*-defective cells

To determine whether DHA plays a role in peroxisome morphogenesis, peroxisome abundance in *AOx*- and *D-BP*-deficient fibroblasts was determined with and without supplementation with DHA. In both types of mutant fibroblasts, growth in culture in the presence of 50 μM DHA for 24 hours resulted in a several-fold increase in the cellular levels of DHA in glycerophopholipids compared with cells cultured in normal medium (Table 1). After 12 hours in the presence of 50 μM DHA, a number of elongated peroxisomes were discernible in *AOx*- and *D-BP*-deficient fibroblasts (Fig. 2Ab,Af, inset), without a significant change in peroxisome abundance (99±29 and 108±35, respectively) compared with the corresponding mock-treated cells (93±30 and 101±37, respectively) (Fig. 2A,B). After 24 hours, however, peroxisome abundance in *AOx*- and *D-BP*-defective fibroblasts increased to 149±56 and 159±60, respectively; at 48 hours, the number of peroxisomes increased to 207±69 and 220±62, respectively (Fig. 2A,B). The increase in peroxisome abundance was dose-dependent, with a higher concentration of DHA (150 μM) being more effective. These results suggested that DHA induces peroxisomal elongation and subsequent peroxisome abundance in a manner that is both time- and dose-dependent. The relationship between peroxisomal elongation and elevated intracellular DHA level was examined over a more detailed time-course (Fig. 2C). After 6–9 hours of DHA treatment, intracellular levels of DHA in *AOx*-deficient fibroblasts were restored to nearly the level seen in control fibroblasts. Intriguingly, there appeared to be concomitant peroxisomal elongation at 6–9 hours. These results suggested that the restoration of intracellular DHA levels is a prerequisite for peroxisomal elongation.

The effect of DHA on normal and *PEX10*-defective fibroblasts was also examined. Supplementation of control fibroblasts with DHA for 48 hours induced peroxisomal elongation without altering the number of peroxisomes (Fig. 2Dc, inset and Fig. 2E), which was similar to the effect on *AOx*- and *D-BP*-defective cells (Fig. 2Ab,Af, inset). This suggested that peroxisome abundance is strictly regulated in normal fibroblasts. *PEX10*-deficient fibroblasts are defective in the import of peroxisomal matrix proteins and contain peroxisomal membrane structures called peroxisomal remnants. DHA supplementation had no effect on peroxisome morphology in *PEX10*-deficient fibroblasts (Fig. 2Db,Dd and Fig. 2E). Essentially the same results were obtained with patient-derived *PEX2*-defective fibroblasts, which were defective in matrix protein transport (Shimozawa et al., 1992b) (Fig. 2E). These findings suggested that matrix proteins are required for DHA-mediated peroxisome proliferation. Thus, supplementation with DHA increased peroxisome abundance in *AOx*- or *D-BP*-deficient fibroblasts via peroxisomal elongation.

To investigate the specificity of the response to DHA, peroxisome abundance in *AOx*-deficient fibroblasts was determined after culture for 48 hours in the presence of various fatty acids. Supplementation with DHA gave rise to the highest number of peroxisomes (187±73), but there were positive, albeit weaker in some cases, effects seen with several other PUFAs. The effect of eicosapentaenoic acid (EPA) on peroxisome abundance was similar to that of DHA (179±60), and there were progressively less potent effects with arachidonic acid (AA; 144±38) and α-linolenic acid (α-LA, 129±43) (supplementary material Fig. S1A). There was no such effect of mono-unsaturated or saturated fatty acids of similar chain length, including oleic acid (OA, 99±31) and stearic acid (96±29). These results suggested that several PUFAs might play an auxiliary role in DHA-induced peroxisomal proliferation.

Free PUFAs, including DHA, are well-characterized ligands of peroxisome proliferator-activated receptor α (PPARα) (Krey et al., 1997). To determine whether DHA induced peroxisomal proliferation via the activation of PPARα, the effects of DHA on peroxisome abundance in PPARα-deficient cells was examined. In cells treated with a small inhibitory RNA (siRNA) targeting *PPARα* (*PPARα*-knockdown cells), DHA induced the proliferation of peroxisomes to the level seen in cells treated with control siRNA (supplementary material Fig. S2A).

Table 1. DHA content in fibroblasts from a normal control and patients with peroxisomal defects

Phospholipids	Control	*PEX10*	*AOx*	*D-BP*	X-ALD	*AOx* + DHA*	*D-BP* + DHA*
PC-DHA	30.8±2.2	21.9±2.3	16.0±2.2	22.2±1.2	38.5±6.1	131.2±16.3	149.3±26.4
ePC-DHA	6.1±0.8	0.3±0.1	3.5±0.7	2.9±0.2	5.6±0.4	9.2±1.2	8.8±0.4
PE-DHA	14.5±1.2	19.3±1.6	6.1±1.8	9.5±1.5	13.8±1.3	44.7±6.2	43.4±0.6
plPE-DHA	48.0±3.2	2.9±0.2	20.2±4.3	20.5±3.4	28.6±3.2	40.0±5.5	41.6±2.5
PS-DHA	0.61±0.05	0.06±0.01	0.38±0.15	0.35±0.02	0.53±0.20	1.04±0.24	1.50±0.41
Total-DHA	100	44.5±3.7	46.1±6.6	55.5±6.1	87.0±5.5	226.1±28.0	244.8±25.2

Values are mol% of the total DHA in control fibroblasts, representing means±s.d. (n=3). PC, phosphatidylcholine; ePC, 1-alkyl-phosphatidylcholine; PE, phosphatidylethanolamine; plPE, plasmenylethanolamine; PS, phosphatidylserine.

*Fibroblasts cultured with 50 μM DHA for 24 hours.

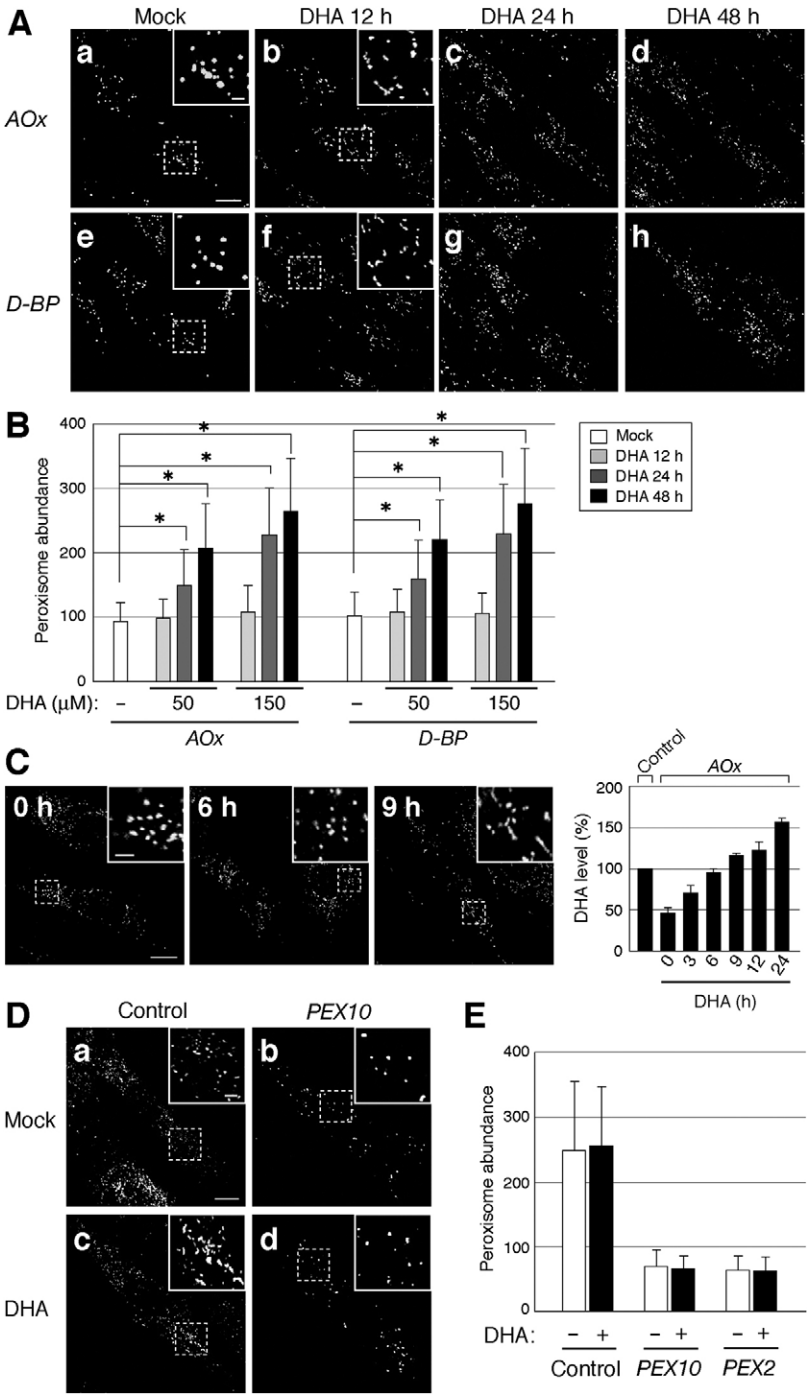

Fig. 2. DHA restores peroxisome morphogenesis in *AOx*- and *D-BP*-defective fibroblasts. (**A**) Fibroblasts defective in *AOx* (Aa–Ad) or *D-BP* (Ae–Ah) were cultured in the absence (Aa,Ae) or presence of 50 μM DHA for 12 hours (Ab,Af), 24 hours (Ac,Ag) or 48 hours (Ad,Ah), and then stained with an antibody to Pex14p. (**B**) Peroxisome abundance per cell following treatment with 50 or 150 μM DHA for the indicated times was determined as described in Materials and Methods. (**C**) *AOx*-deficient fibroblasts were cultured with 50 μM DHA for 0, 3, 6, 9, 12 and 24 hours. Peroxisome morphology was verified using an antibody to Pex14p (left panel). Total DHA levels were analyzed as described for Table 1 (right panel). Values are mol% of total DHA in control fibroblasts. (**D**) Control (Da,Dc) or *PEX10*-deficient (Db,Dd) fibroblasts were cultured in the absence (Da,Db) or presence (Dc,Dd) of 150 μM DHA for 48 hours and then stained with an antibody to Pex14p. (**E**) Fibroblasts from control and individual patients defective in *PEX10* and *PEX2* were treated with DHA as in A and peroxisome abundance determined. Insets are higher-magnification images of the boxed regions. Scale bars: 10 μm and 2 μm (insets). Data represent the means ± s.d. of three independent experiments; *$P<0.05$.

Moreover, peroxisome abundance was not elevated in control or *AOx*-deficient patient fibroblasts by treatment with the PPARα activator Wy-14,643 (supplementary material Fig. S2B). This was in contrast to the effect of Wy-14,643 on the peroxisome proliferation in mouse embryonic fibroblasts (MEFs). These results suggested that DHA-induced peroxisomal proliferation is independent of PPARα activation.

DLP1 is required for DHA-mediated peroxisome division

Factors involved in peroxisome division are classified into two types: peroxisome-specific factors such as Pex11p, and those common to peroxisomes and mitochondria, including Fis1, DLP1, and mitochondrial fission factor (Gandre-Babbe and van der Bliek, 2008; Kobayashi et al., 2007; Koch et al., 2003; Koch et al., 2005; Li and Gould, 2003; Tanaka et al., 2006; Waterham et al., 2007). Fission mediated by DLP1 is believed to be the final stage in peroxisome division (Koch et al., 2003; Li and Gould, 2003). To assess whether DLP1 was required for DHA-induced peroxisomal proliferation, we turned to a cell-permeable chemical inhibitor of dynamin, called dynasore, which is reported to inhibit the GTPase activity of DLP1 in vitro (Macia et al., 2006). Before testing the inhibitory effect of dynasore in vivo, we

first examined whether dynasore interfered with fragmentation of mitochondria. In normal fibroblasts, exposure to H_2O_2 induced mitochondrial fragmentation (supplementary material Fig. S3), in good agreement with an earlier report (Yoon et al., 2006). However, in the presence of 40 μM dynasore, mitochondrial fragmentation was strongly suppressed, which indicated that dynasore inhibited DLP1 in vivo. To determine whether inhibition of DLP1 affected DHA-induced peroxisomal proliferation, the number and morphology of peroxisomes in *AOx*-deficient fibroblasts were examined in the presence and absence of dynasore. In the absence of DHA supplementation, peroxisome abundance and morphology were not altered by dynasore treatment (Fig. 3Aa,Ab and Fig. 3B). By contrast, in DHA-pretreated cells, peroxisomal proliferation was inhibited by dynasore (Fig. 3Ac,Ad). As shown in Fig. 3B, the number of peroxisomes in dynasore-treated fibroblasts was 95±33, similar to that seen in control DMSO-treated fibroblasts (98±31). The increase in peroxisome abundance in DHA-treated cells was significantly reduced by dynasore compared with mock-treated cells (128±67 vs 246±84, respectively). Moreover, *DLP1* knockdown significantly inhibited the DHA-induced increase in peroxisome abundance in *AOx*-defective fibroblasts, resulting in numerous elongated peroxisomes (Fig. 3C–E). Collectively, these results indicated that DHA induces peroxisomal division via DLP1-mediated fission.

DLP1 is translocated to the peroxisomal or mitochondrial membrane to promote the fission of these organelles (Kobayashi et al., 2007; Koch et al., 2003; Li and Gould, 2003; Pitts et al., 1999; Tanaka et al., 2006). We next investigated the localization of DLP1 in *AOx*-deficient fibroblasts by immunofluorescence microscopy. DLP1 was localized to peroxisomes in the absence or presence of DHA (Fig. 3F), which suggested that the translocation of DLP1 is not affected by DHA. Moreover, mitochondrial morphology was not altered in cells impaired in peroxisomal β-oxidation, even after treatment with DHA (data not shown). These results suggested that DHA modulates peroxisome-specific factors to induce peroxisomal division.

DHA induces peroxisome elongation and division in a Pex11p-dependent manner

We next investigated whether DHA-mediated peroxisomal elongation and proliferation were dependent on the peroxisome-specific division factor Pex11p. In mammalian cells, there are three isoforms of *PEX11*, namely *PEX11α*, *PEX11β* and *PEX11γ*, of which at least two (*PEX11α* and *PEX11β*) are expressed in human cells (Abe and Fujiki, 1998; Abe et al., 1998; Schrader et al., 1998). Treatment of *AOx*-deficient fibroblasts with siRNAs targeting *PEX11α* and *PEX11β* resulted in significant decreases in *PEX11β* and *PEX11α* mRNA, respectively (Fig. 4B and supplementary material Fig. S4B). DHA had no effect on peroxisome elongation at 12 hours or on division at 24 hours in *PEX11β*-knockdown fibroblasts (Fig. 4A–C), which strongly suggested that Pex11pβ-mediated elongation is a prerequisite for peroxisome fission. By contrast, in *PEX11α*-knockdown cells, peroxisome elongation was apparent at 12 hours, similar to that seen in control siRNA-treated cells. Peroxisome number, on the other hand, was slightly lower at 24 hours and was approximately 70% of that seen in control siRNA-treated cells (supplementary material Fig. S4A–C). These results indicated that DHA-mediated peroxisome division is mediated in part by Pex11pα. Thus, DHA-mediated

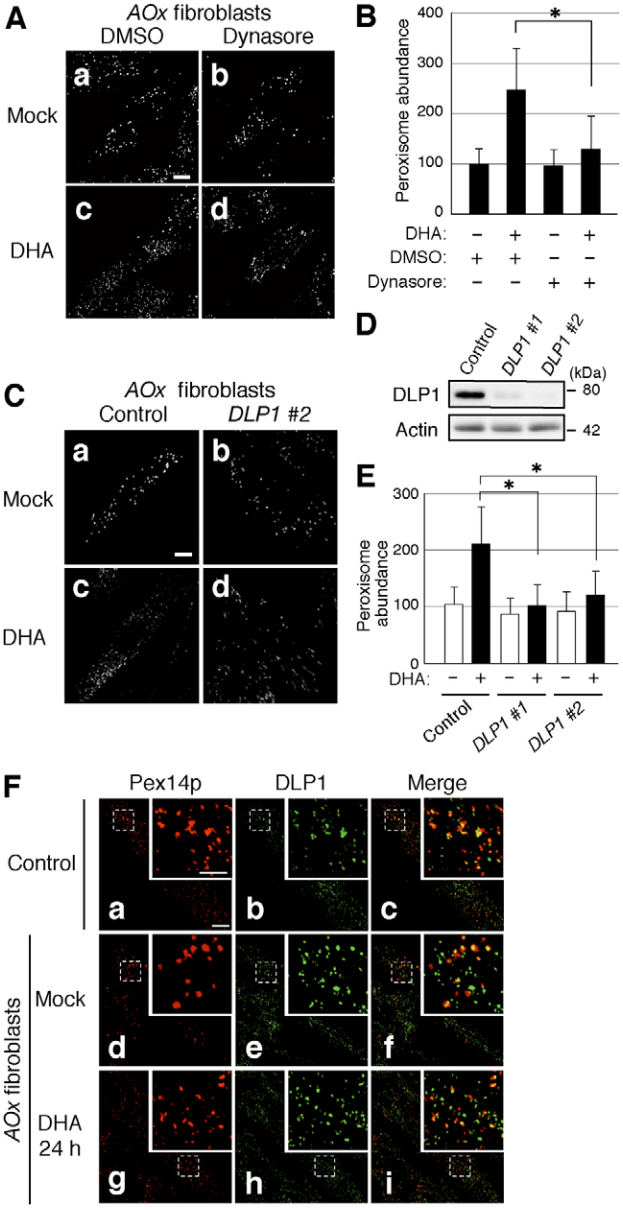

Fig. 3. Functional role of DLPI in peroxisome proliferation. (**A**) *AOx*-deficient fibroblasts were cultured for 16 hours in the absence (Aa,Ab) or presence (Ac,Ad) of 150 μM DHA and then treated for an additional 8 hours with DMSO (Aa,Ac) or 40 μM dynasore (Ab,Ad). Cells were stained with an anti-Pex14p antibody. (**B**) Peroxisome abundance per cell was determined as in Fig. 2B. (**C**) *AOx*-deficient fibroblasts were treated for 48 hours with a control dsRNA (left panel) or *DLP1* #2 dsRNA (right panel). Cells were cultured for an additional 24 hours in the absence (Ca,Cb) or presence (Cc,Cd) of 150 μM DHA and then stained with an anti-Pex14p antibody. (**D**) *AOx*-deficient fibroblasts were treated for 48 hours with a control dsRNA or two different test dsRNAs (*DLP1* #1 and *DLP1* #2). DLP1 levels were verified by immunoblot analysis using an anti-DLP antibody. Actin was used as a loading control. (**E**) Peroxisome abundance per cell was determined as in Fig. 2B. (**F**) Control (Fa–Fc) and *AOx*-deficient fibroblasts (Fd–Fi) were cultured for 24 hours in the absence (Fa–Ff) or presence (Fg–Fi) of 150 μM DHA. Cells were stained with antibodies to Pex14p (Fa,Fd,Fg) and DLP1 (Fb,Fe,Fh); the merged view of the two different proteins is shown in Fc, Ff, and Fi. Insets are higher-magnification images of the boxed regions. Scale bars: 10 μm and 2 μm (insets). Data represent the means ± s.d. of three independent experiments; $*P<0.01$.

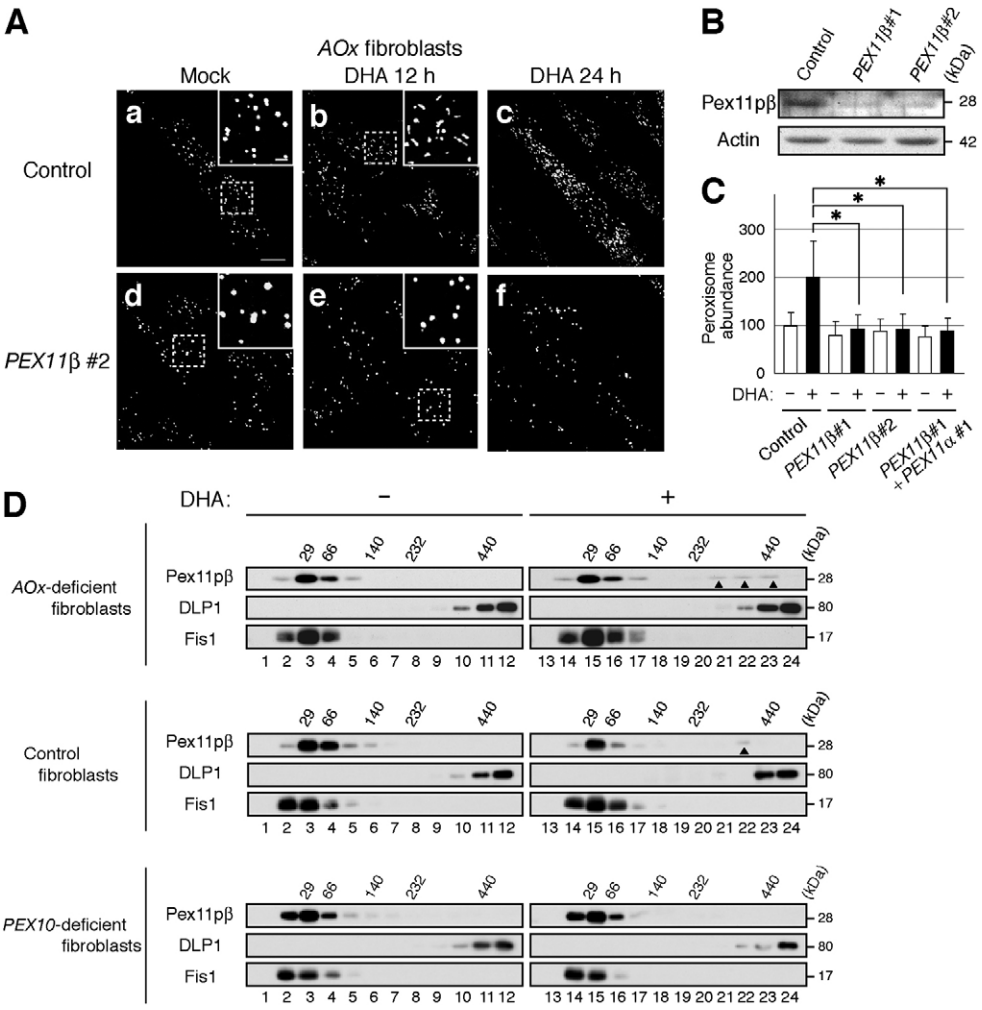

Fig. 4. DHA induces peroxisome elongation and division in a Pex11pβ-dependent manner. (**A**) *AOx*-deficient fibroblasts were treated with a control dsRNA (upper row) or *PEX11β* #2 dsRNA (lower row) for 48 hours. Cells were cultured for an additional 12 hours (Ab,Ae) and 24 hours (Aa,Ac,Ad,Af) in the absence (Aa,Ad) or presence (Ab,Ac,Ae,Af) of 150 μM DHA and then stained with an anti-Pex14p antibody. Insets are higher-magnification images of the boxed regions. Scale bars: 10 μm and 2 μm (insets). (**B**) *AOx*-deficient fibroblasts were treated with control dsRNA or two different test dsRNAs (*PEX11β* #1 and *PEX11β* #2) for 48 hours. Pex11pβ levels were verified by immunoblot analysis using an antibody to Pex11pβ. Actin was used as a loading control. (**C**) *AOx*-deficient fibroblasts were treated as in A with control, *PEX11β* #1, *PEX11β* #2 or *PEX11β* #1 plus *PEX11α* #1 dsRNAs. Cells were cultured for an additional 24 hours in the absence or presence of 150 μM DHA. Peroxisome abundance per cell was determined as in Fig. 2B. Data represent the means ± s.d. of three independent experiments; **P*<0.01. (**D**) *AOx*-deficient, control, and *PEX10*-deficient fibroblasts were cultured for 20 hours in the absence (left panels) or presence (right panels) of 150 μM DHA and then treated for 30 minutes with 1 mM DSP. Cell lysates were fractionated by sucrose density gradient ultracentrifugation and each fraction analyzed by immunoblot using antibodies to Pex11pβ, DLP1 and Fis1. Upward arrowhead indicates the higher molecular-mass oligomer of Pex11pβ.

peroxisomal proliferation appears to depend, either wholly or partly, on Pex11pα and Pex11pβ.

The N-terminal domain of Pex11pβ is required for homo-oligomerization and is indispensable for its ability to stimulate peroxisomal proliferation (Kobayashi et al., 2007). To investigate whether the oligomeric state of Pex11pβ was affected by DHA, protein oligomerization was assessed by sucrose-density gradient fractionation. *AOx*-deficient fibroblasts cultured in the presence or absence of DHA were treated with a crosslinker, dithiobis[succinimidyl propionate] (DSP) and then solubilized with 1% Triton X-100, followed by ultracentrifugation in a sucrose-density gradient. In the absence of DHA, Pex11pβ sedimented with a mass of approximately 29 kDa, corresponding to the monomeric form (Fig. 4D, top left panel). By contrast, DHA supplementation gave rise to high molecular mass complexes of Pex11pβ ranging from 230 to 430 kDa, in addition to the native 29-kDa form (Fig. 4D, top right panel, upward arrowheads). The sizes of the molecular complexes of DLP1 and Fis1, which interact with Pex11pβ, were not altered by DHA supplementation. Moreover, a higher mass oligomer of Pex11pβ was detected in control fibroblasts, but not in *PEX10*-defective fibroblasts, in the presence of DHA (Fig. 4D, middle and bottom panels). This apparent oligomeric transition correlated with the effect of DHA on peroxisome elongation, a prerequisite for peroxisomal proliferation (Fig. 2A,D). Collectively, these results suggested that DHA induces peroxisome elongation through augmentation of Pex11pβ oligomerization. The oligomeric state of Pex11pβ was also examined in *AOx*-deficient fibroblasts cultured in the presence of several other PUFAs that induced peroxisomal proliferation to varying degrees (supplementary

material Fig. S1A). In addition to DHA, both EPA and α-LA enhanced the oligomerization of Pex11pβ (supplementary material Fig. S1B), suggesting that these other PUFAs exert their auxiliary effects on peroxisomal proliferation via effects on Pex11pβ oligomerization.

The role of Pex11pβ oligomerization was further examined in an in vitro assay using synthetic proteoliposomes. The peroxisomal membranes of rat reportedly contain a high level of DHA; approximately 25% of total phosphatidylcholine (PC) and phosphatidylethanolamine (PE) contain DHA (Yang et al., 2003). In mouse liver peroxisomes, DHA-containing PC levels are elevated upon treatment with clofibrate, a peroxisome proliferator (Crane and Masters, 1986). Three types of liposomes, standard liposomes (SL), DHA-enriched liposomes (DL) and oleic acid-enriched liposomes (OL), were reconstituted with recombinant Pex11pβ fused to maltose binding protein (MBP). As shown in Fig. 5A, DL contained the highest level of DHA (43% of total phospholipids), whereas SL and OL contained a much lower level of DHA (4–8% of total phospholipids). Proteoliposomes were solubilized with 1% Triton X-100 and then analyzed by ultracentrifugation in a glycerol-density gradient. High molecular mass complexes of MBP–Pex11pβ were markedly increased in DL as compared with SL and OL (Fig. 5B). These results strongly suggested that DHA-containing phospholipids directly augment homo-oligomerization of Pex11pβ.

To begin to elucidate the mechanism of peroxisome elongation into tube-like structures, the localization of Pex11pβ along elongated peroxisomes was examined in *AOx*-deficient fibroblasts in the absence and presence of DHA. After 12 hours in the presence of DHA, Pex11pβ and Pex14p localized to mutually exclusive regions on elongated peroxisome structures (Fig. 6A,B). By contrast, in mock-treated cells, there was extensive colocalization of Pex11pβ and Pex14p (Fig. 6Aa–Ac). Moreover, the patterns of staining of 70-kDa peroxisomal membrane protein (PMP70) and catalase (typical peroxisomal membrane and matrix proteins, respectively) were superimposable on that of Pex14p in the absence or presence of DHA (Fig. 7A,B). These results indicated that DHA supplementation gives rise to distinct Pex11pβ-enriched regions on peroxisomal membranes and that these complexes mediate peroxisomal elongation.

Peroxisome division is not regulated by Pex16p-AOx complexes in mammalian cells

Pex16p negatively regulates peroxisomal division in the yeast *Yarrowia lipolytica* (Guo et al., 2007). Interaction of Pex16p with AOx inside the peroxisome relieves this negative regulation and promotes peroxisome division (Guo et al., 2007). To investigate whether the abnormal morphogenesis of peroxisomes in *AOx*-deficient fibroblasts was due to defects in Pex16p–AOx complexes, peroxisome abundance was examined in *AOx*-deficient fibroblasts treated with an siRNA targeting *PEX16*. In contrast to the excessive peroxisomal proliferation observed in *PEX16*-knockdown *Y. lipolytica* (Guo et al., 2007), *PEX16* knockdown had no effect on peroxisome morphology in *AOx*-fibroblasts, as assessed 72 hours after siRNA treatment (supplementary material Fig. S5). These results suggested that peroxisome division is not regulated by Pex16p–AOx complexes in mammalian cells, and that there is a different regulatory mechanism for peroxisomal proliferation in mammalian cells.

Real-time imaging of peroxisome division

Peroxisome division involves elongation of peroxisomes followed by subsequent fission (Koch et al., 2003; Li and Gould, 2003; Schrader et al., 1998). However, the steps in peroxisome division have yet to be clearly demonstrated. To delineate the stages of peroxisome division, *AOx*-deficient fibroblasts were transfected with an expression construct for the tripeptide AKL fused to green fluorescent protein (EGFP) and hemagglutanin (HA) (*HA_2-EGFP-AKL*). Transfected cells were cultured in the presence of DHA for 20 hours and then monitored by time-lapse fluorescence microscopy. Dividing peroxisomes were readily detected as morphologically fluid structures, undergoing repeated rounds of elongation and contraction followed by membrane fission (Fig. 8A; see also supplementary material Movie 1). Furthermore, peroxisomal membranes appeared to extend from one side of the structure (Fig. 8B; see supplementary material Movie 2), consistent with a recent report (Delille et al., 2010). These results clearly demonstrated the sequence of steps involved in peroxisome division, i.e. elongation in one direction followed by fission.

Microtubule assembly is required for proper distribution of divided peroxisomes

Microtubule-based peroxisome trafficking is suggested to be essential for the proper intracellular distribution of peroxisomes in mammalian cells (Wiemer et al., 1997). Treatment of cells with nocodazole, a microtubule depolymerization agent, resulted in peroxisome clustering in *AOx*-deficient fibroblasts cultured in the presence of DHA (Fig. 9A, arrows), which suggested that rapid translocation of divided peroxisomes along microtubules is required for proper intracellular distribution. However, nocodazole did not appear to modify peroxisomal elongation

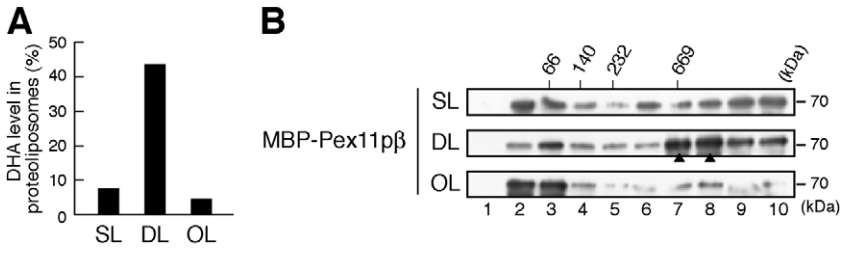

Fig. 5. In vitro Pex11pβ oligomerization assay. (**A**) DHA levels in proteoliposomes. SL were prepared by mixing PC and PE. DL were prepared by mixing PDPC and PDPE, and OL by mixing POPC and POPE. DHA levels were determined as described in Materials and Methods. (**B**) Introduction of an MBP–Pex11pβ fusion protein into liposomes. Liposomes were solubilized with 1% Triton X-100 and then fractionated by ultracentrifugation in a 1–30% glycerol density gradient. Each fraction was analyzed by immunoblot using an anti-MBP antibody. Upward arrowheads indicate the higher molecular mass oligomers of MBP–Pex11pβ.

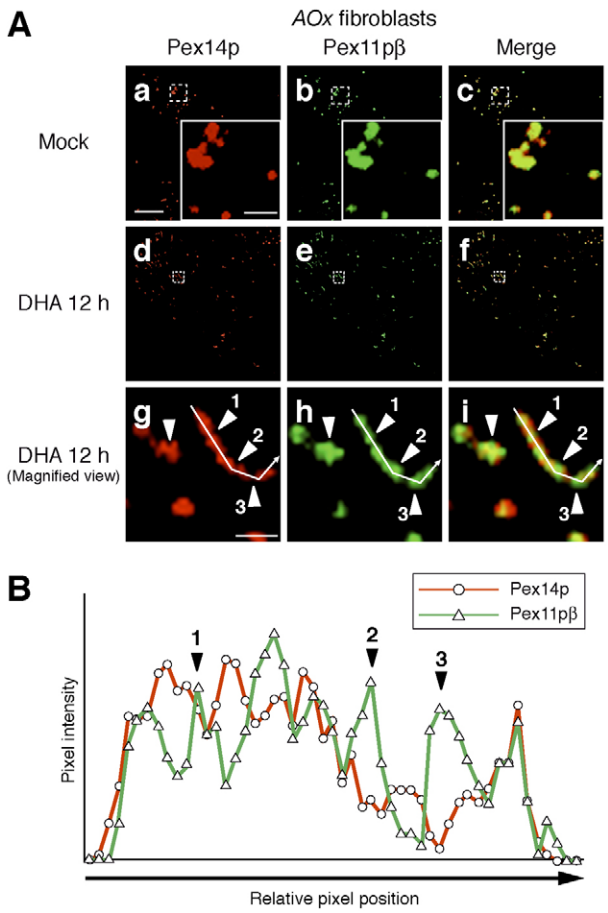

Fig. 6. DHA induces the formation of Pex11pβ-rich regions on elongated peroxisomes. (**A**) *AOx*-deficient fibroblasts were cultured in the absence (Aa–Ac) or presence (Ad–Ai) of 150 μM DHA for 12 hours and then stained with antibodies to Pex14p (Aa,Ad,Ag) and Pex11pβ (Ab,Ae,Ah); the merged view of the two proteins is shown in Ac, Af and Ai. Insets are higher-magnification images of the boxed regions. Scale bars: 10 μm and 1 μm (insets). Arrowheads indicate regions enriched with Pex11pβ compared with Pex14p. The numbers 1, 2 and 3 correspond to those in panel B. (**B**) Mutually distinct peaks of Pex11pβ and Pex14p were apparent upon in-line scanning of the transecting line shown in Ag–Ai. The intensity of Pex11pβ signals was significantly increased at regions (arrowheads) that did not contain Pex14p.

and division (Fig. 9A,B). Taken together, the results indicate that association with microtubules is required for proper distribution of newly divided peroxisomes, but is not required for division per se.

Discussion

Peroxisome function is maintained by normal peroxisomal biogenesis, the generally accepted model for which is called ‘growth and division’ (Lazarow and Fujiki, 1985). Impaired matrix protein import (a ‘growth’ defect) results in typical peroxisomal dysmorphogenesis, most probably due to the resultant defect in ‘division’ (Chang et al., 1999; Santos et al., 1988). Impaired peroxisomal fatty acid β-oxidation is also suggested to cause dysmorphogenesis of peroxisomes (Chang et al., 1999; Funato et al., 2006). Results from the current study (Fig. 1) were consistent with these previous observations, and suggested that peroxisomal metabolites may be involved in peroxisomal morphogenesis. However, the mechanisms underlying this impaired morphogenesis are largely undefined.

The levels of DHA-containing phospholipids such as PC and plasmenylethanolamine were approximately 50% lower in fibroblasts with altered peroxisome morphogenesis (Table 1). Supplementation with DHA restored DHA-containing phospholipids to normal or higher levels (Table 1) and restored proper peroxisome structure (Fig. 2). These results strongly suggested that DHA is an inducer of peroxisomal division. DHA induced the elongation and subsequent fission of peroxisomes in a Pex11p-dependent manner, indicating that DHA is essential for peroxisome division. Peroxisome division was augmented by several other PUFAs to varying extents (supplementary material Fig. S1A,B), suggesting that these PUFAs also function as potent inducers of peroxisomal division. However, the intracellular levels of several fatty acids, including EPA and AA, in *AOx*- and *D-BP*-deficient fibroblasts were similar to those in control fibroblasts (supplementary material Fig. S1C). This was in contrast to the significantly reduced levels of DHA in *AOx*- and *D-BP*-deficient fibroblasts (Table 1). Moreover, in mouse liver peroxisomes, PC-DHA is elevated upon treatment of the mouse with clofibrate, a peroxisomal proliferator, with no significant alteration of the levels of PC-AA (Crane and Masters, 1986). On the basis of these results, we propose that peroxisome division is specifically mediated by DHA under physiological conditions.

Pex11pβ is implicated as a crucial factor in peroxisome division. We have provided several lines of evidence that Pex11pα and Pex11pβ regulate peroxisome elongation, the initiation step in peroxisome division (Fig. 4 and supplementary material Fig. S4). Knockdown of *PEX11α* significantly attenuated DHA-mediated peroxisome proliferation, although less severely than knockdown of *PEX11β* (Fig. 4 and supplementary material Fig. S4). Of note, there were no apparent phenotypic differences between single-knockdown *PEX11β* fibroblasts and double-knockdown *PEX11α*/*PEX11β* fibroblasts (Fig. 4C). These results indicate that Pex11pβ plays a key role in peroxisomal division, and that Pex11pα plays an auxiliary role to Pex11pβ. Previous studies have shown that PPARα induces the expression of *PEX11α*, but not *PEX11β* (Li et al., 2002a; Schrader et al., 1998; Shimizu et al., 2004). Accordingly, Pex11pα most probably increases peroxisome abundance as part of the cellular response to various stimuli.

Recently, Koch and colleagues reported that another isoform of Pex11p, Pex11pγ, coordinates peroxisome division via an interaction with Pex11pα or Pex11pβ (Koch et al., 2010). *PEX11β* is expressed in almost all types of human cells (Schrader et al., 1998). By contrast, *PEX11α* and *PEX11γ* are expressed in a tissue-specific manner (Li et al., 2002a; Schrader et al., 1998). Thus, elucidating the function Pex11pβ is an important step towards a full understanding of the fundamental mechanisms of peroxisome division.

Several techniques for inducing the elongation and proliferation of peroxisomes have been reported. Overexpression of Pex11pβ gives rise to high levels of peroxisome proliferation (Kobayashi et al., 2007; Li and Gould, 2002; Schrader et al., 1998), similar to treatment with peroxisome proliferators such as clofibrate (Crane and Masters, 1986) and 4-phenylbutyrate (Gondcaille et al., 2005; Kemp et al., 1998; Wei et al., 2000). Ectopic expression of a dominant-negative form of DLP1 results in the accumulation of elongated peroxisomes (Koch et al., 2003; Li and Gould, 2003; Tanaka et al., 2006), similar to that observed in a *dlp1* mutant CHO cell line (Tanaka et al., 2006) and in fibroblasts from patients with

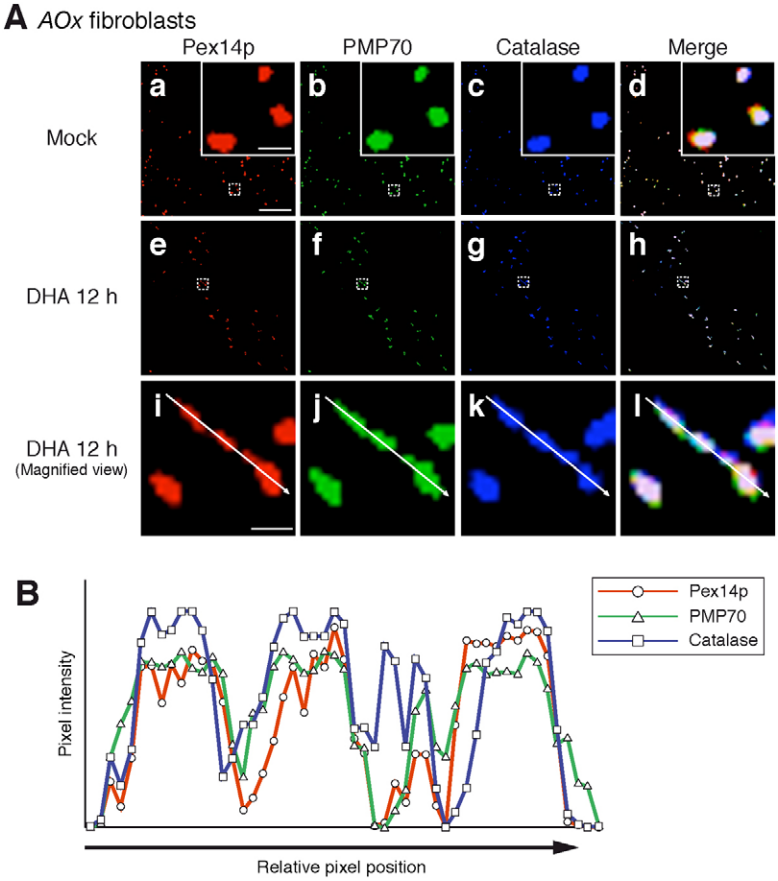

Fig. 7. PMP70 and catalase colocalize with Pex14p. (**A**) *AOx*-deficient fibroblasts were cultured in the absence (Aa–Ad) or presence (Ae–Al) of 150 µM DHA for 12 hours and then stained with antibodies to Pex14p (Aa,Ae,Ai), PMP70 (Ab,Af,Aj), and catalase (Ac,Ag,Ak); the merged view of the proteins is shown in Ad, Ah and Al. Scale bars: 10 µm and 1 µm (insets). (**B**) Line-scanning evaluation of the transecting line shown in Ai–Al. Note the similar peaks for Pex14p, PMP70 and catalase. Insets are higher-magnification images of the boxed regions.

impaired DLP1 function (Waterham et al., 2007). Recently, Delille and colleagues showed that overexpression of a Pex11pβ–YFP fusion protein results in peroxisome elongation, but no division (Delille et al., 2010). Importantly, the results highlight the utility of fluorescent Pex11pβ–YFP as a tool for delineating the elongation step of peroxisome division. However, the observed accumulation of tubular peroxisomes might not reflect, or only partially reflect, the bona fide physiological functions of Pex11pβ. With the current experimental system of DHA-induced peroxisome division, distinct elongation and fission steps of peroxisomal proliferation were readily apparent under physiological conditions, without changes in the expression levels of *PEX11α* and *PEX11β* (supplementary material Fig. S2C). Thus, for the first time, we have been able to address the functional role of endogenous Pex11pβ in peroxisome division.

Delille et al. recently reported that ectopic expression of Pex11pβ promotes the extension of Pex11pβ-enriched membranes and the segregation of Pex11pβ from other peroxisomal proteins (Delille et al., 2010), which is similar to previous reports (Koch et al., 2010; Schrader et al., 1998). Pex11pβ appears to form or localize to regions that are distinct from those harboring common membrane proteins. In the present work, we observed the formation of multiple Pex11pβ-enriched regions on elongated peroxisomes as well as extensions of Pex11pβ-enriched membranes in response to DHA (Fig. 6). These results suggest that, during peroxisome division, Pex11pβ functions in two distinct processes: membrane elongation and the creation of multiple regions for segregation of parent and daughter peroxisomes.

The molecular mechanisms underlying the modulation of peroxisome morphogenesis by Pex11pβ remain elusive. During peroxisome division, DHA augmented the oligomerization of Pex11pβ and induced the elongation of peroxisomes by facilitating the creation of multiple Pex11pβ-enriched regions on peroxisomal membranes (Figs 4, 6). The regulation of peroxisome division by monomeric or oligomeric forms of Pex11p is preserved from yeast to humans (Kobayashi et al., 2007; Marshall et al., 1996). In mammalian cells, Pex11pβ interacts with DLP1 and Fis1, and homo-oligomerization of Pex11pβ in particular is indispensable for peroxisome division (Kobayashi et al., 2007). The present study showed that DHA modulated the monomer-to-oligomer transition of Pex11pβ, but not DLP1 and Fis1 (Fig. 4D). It is important to note, however, that the transition of DLP1 and Fis1 to higher molecular mass hetero-oligomeric complexes with Pex11pβ might not be readily detectable at endogenous levels. Moreover, the results of the in vitro Pex11pβ oligomerization assay demonstrated that DHA can directly induce homo-oligomerization of Pex11pβ (Fig. 5). These findings suggest that DHA augments the homo-oligomerization of Pex11pβ, thereby inducing elongation and fission of peroxisomes.

The effects of DHA on control fibroblasts were also characterized. DHA augmented the oligomerization of Pex11pβ in control as well as *AOx*-deficient fibroblasts (Fig. 4D). However, in contrast to *AOx*-deficient fibroblasts, DHA induced only the elongation, and not the fission of peroxisomes in control fibroblasts (Fig. 2D,E). Thus, it appears that the oligomerization of Pex11pβ gives rise to peroxisome elongation. At present, we do

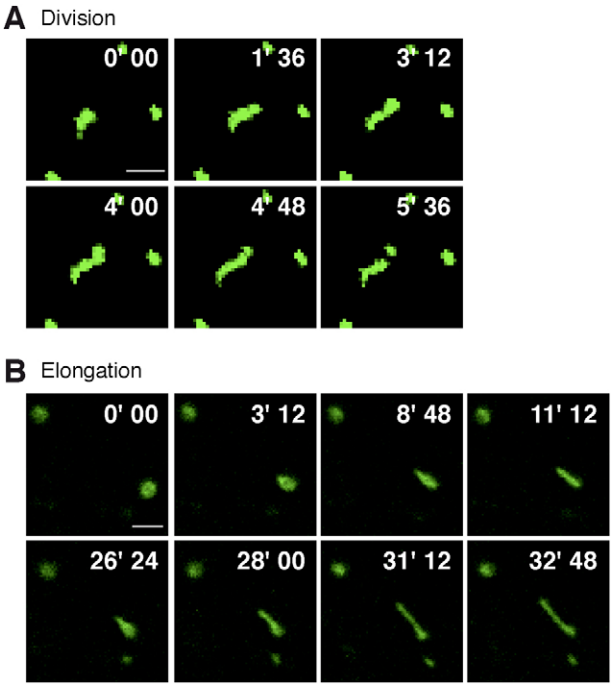

Fig. 8. Real-time imaging of peroxisome division. (**A**,**B**) *AOx*-deficient fibroblasts were transfected with an expression vector for *HA*$_2$*-EGFP-AKL*. After 4 hours, fibroblasts were supplemented with 150 μM DHA for 20 hours and then analyzed by time-lapse fluorescence microscopy. Images show division (A) and the sequence of steps involved in peroxisome elongation (B). Scale bar: 1 μm.

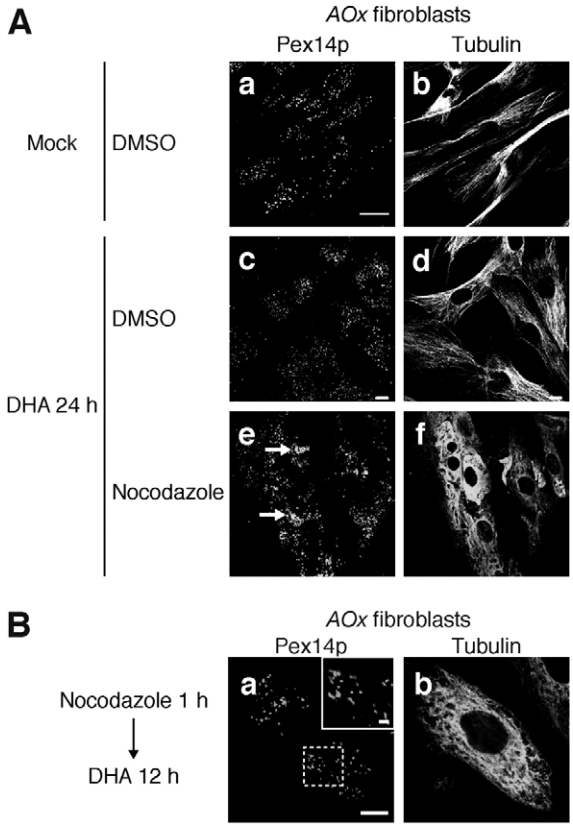

Fig. 9. Association of peroxisomes with microtubules is required for proper distribution but not division. (**A**) *AOx*-deficient fibroblasts were cultured for 4 hours in the absence (Aa,Ab) or presence of 150 μM DHA (Ac–Af) followed by the addition of DMSO (Aa–Ad) or 10 μM nocodazole (Ae,Af) for 20 hours. Cells were stained with antibodies to Pex14p (Aa,Ac,Ae) and α-tubulin (Ab,Ad,Af). Arrows indicate peroxisomal clusters. Scale bars: 20 μm. (**B**) Microtubules are not involved in peroxisomal elongation. *AOx*-deficient fibroblasts were treated with 10 μM nocodazole for 1 hour and then cultured for 12 hours in the presence of 150 μM DHA. Cells were stained with antibodies to Pex14p (Ba) and α-tubulin (Bb). Insets are higher-magnification images of the boxed regions. Scale bars: 10 μm and 2 μm (inset).

not know why peroxisomes remain at the elongation step in normal fibroblasts and do not proceed to the fission stage. It underscores what is probably a complex mechanism by which peroxisome abundance is strictly maintained at a constant level under normal conditions.

What is the physiological consequence of the elongation of peroxisomes? Peroxisome elongation is regarded as the first step of peroxisome proliferation, followed by fission mediated by DLP1 (Koch et al., 2003; Li and Gould, 2003; Schrader et al., 1998; Tanaka et al., 2006). In *AOx*-deficient fibroblasts, DLP1 localized to peroxisomes (Fig. 3F), despite the fact that division was compromised in these cells. These results suggest that DLP1 is in an inactive state on the morphologically abnormal peroxisomes. Given that DHA supplementation promoted peroxisome division in *AOx*-defective fibroblasts, DHA-mediated elongation might be a prerequisite for the activation of DLP1. Interestingly, the yeast DLP1 homolog Dnm1 forms narrow spirals with a diameter of approximately 100 nm during membrane fission (Ingerman et al., 2005). The diameter of the hypertrophic peroxisomes in *AOx*- or *D-BP*-deficient fibroblasts is over 200 nm (Funato et al., 2006), more than twice the diameter of Dnm1 spirals. Thus it seems unlikely that DLP1 forms the appropriate spiral on morphologically aberrant peroxisomes. DHA induced the formation of Pex11pβ-enriched and membrane-constricted regions along elongated peroxisome that were devoid of Pex14p (Fig. 6). In fact, these membrane-constricted regions are reported to be approximately 100 nm in diameter (Koch et al., 2004). Thus, these DHA-induced regions of constriction along the elongated peroxisomes that are highly enriched in Pex11pβ might facilitate the formation of the spiral DLP1 structures necessary for peroxisome fission.

The underlying mechanism by which DHA mediates peroxisomal proliferation could include PPARα activation. In DHA-treated cells, decreased cellular levels of PC and PE that contain PUFAs other than DHA were apparent, in contrast to the increase in DHA-containing phospholipids (data not shown), which suggests that PUFAs are released by remodeling of phospholipids (Shimizu et al., 2006; Shindou and Shimizu, 2009). It is well known that free PUFAs, including DHA, are ligands for PPARα (Krey et al., 1997). However, in the current study, DHA induced peroxisomal division in a manner that was independent of *PPARα* activation (supplementary material Fig. S2A,B). An intriguing possibility is that lipid remodeling in peroxisomal membranes is required for DHA-mediated peroxisome division. An increase in DHA-containing phospholipids is observed in peroxisomal membranes isolated from the liver of mice treated with clofibrate, a hypolipidemic agent and known peroxisome proliferator (Crane and Masters, 1986). In the present study,

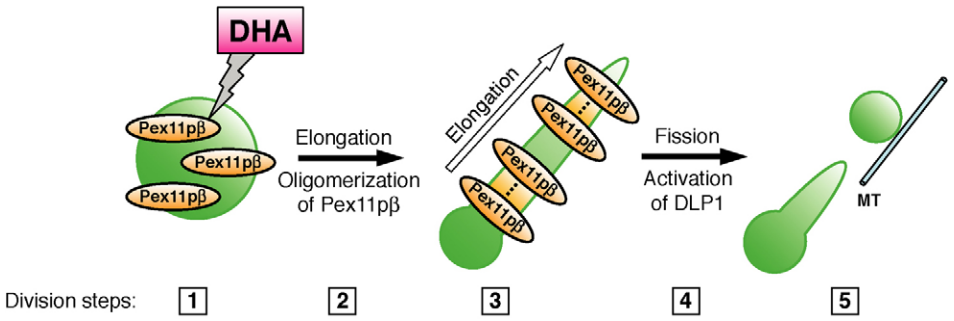

Fig. 10. Model of DHA-mediated peroxisome division. DHA promotes the oligomerization of Pex11pβ, which leads to the formation of Pex11pβ-rich regions and initiates peroxisome elongation (steps 1 and 2), in which peroxisomes elongate in one direction (step 3). The elongation of peroxisomes activates DLP1 to cleave peroxisomal membranes, thereby giving rise to peroxisomal fission (step 4). After division, daughter peroxisomes translocate via microtubules (MT) (step 5). See Discussion for details.

DHA-containing phospholipids directly augmented the oligomerization of Pex11pβ (Fig. 5). These results suggest that the incorporation of DHA into peroxisomal membranes gives rise to the peroxisome division.

The primary sequence of Pex11p of *Saccharomyces cerevisiae* is highly similar to that of the ligand-binding domain of PPAR family members (Barnett et al., 2000). The ligand-binding domain of lipid-activated transcription factors of the PPAR family binds various fatty acids, including PUFAs (Krey et al., 1997). Our results suggest that Pex11pβ directly binds DHA and other similar PUFAs contained within phospholipids in the peroxisomal membrane, consistent with the finding that several PUFAs elevate peroxisome abundance similarly to DHA (supplementary material Fig. S1). Thus, DHA incorporated into the peroxisomal membrane most probably enhances the functional activity of Pex11pβ.

In the current study, DHA, a metabolite of peroxisomes, was identified as a novel mediator of peroxisomal morphogenesis. In *Y. lipolytica*, Pex16p negatively regulates peroxisome division (Guo et al., 2007). Interaction of Pex16p with AOx inside the peroxisome alleviates this negative regulation, giving rise to peroxisome division (Guo et al., 2007). In *Y. lipolytica*, uptake of sufficient amounts of AOx into peroxisomes is a signal for maturation, and only mature peroxisomes are competent for division. A similar maturation signal has yet to be identified in mammalian cells. In contrast to the excessive peroxisomal proliferation observed in *PEX16*-knockdown *Y. lipolytica* (Guo et al., 2007), *PEX16* knockdown did not result in any morphological alterations of peroxisomes in human fibroblasts, even at 72 hours after siRNA treatment (supplementary material Fig. S5), indicating that mammalian cells possess a different mechanism of regulation of peroxisomal division. During DHA biosynthesis, peroxisomal β-oxidation is essential for the last step of the conversion of tetracosahexaenoic acid (C24:6n-3) to DHA. One possibility is that peroxisomal import of sufficient β-oxidation enzymes and a threshold level of DHA-containing phospholipids serve as signals for peroxisome maturation and subsequent division. Thus, DHA could serve as a signal for the completion of the peroxisome growth stage and initiation of subsequent division stages in mammalian cells.

Microtubule assembly was required for the transport of newly divided peroxisomes, but not for division per se, a conclusion based on the effects of the microtubule depolymerization agent nocodazole on peroxisome proliferation (Fig. 9). Recently, it was shown that peroxisomes also associate with the actin cytoskeleton in mammalian cells (Schollenberger et al., 2010), although this association does not appear to be necessary for the movement of peroxisomes (Wiemer et al., 1997). The current results begin to address the functional role of actin fibers in peroxisome division. DHA-induced peroxisome division required at least 8 hours for elongation and 24 hours for proliferation. By comparison, treatment with the actin depolymerization agents cytochalasin B and latrunculin B at the effective concentrations resulted in dramatic changes in cell structures within 3 hours. To determine whether actin polymerization was required for the maintenance of elongated peroxisomes, *AOx*-deficient fibroblasts were cultured for 12 hours in the presence of 150 μM DHA and then treated with cytochalasin B for 3 hours. Elongated peroxisomes persisted in cytochalasin-B-treated cells (data not shown), suggesting that actin polymerization is not involved in peroxisome division, or at least not involved in maintaining peroxisome elongation.

The sequential steps of peroxisome division revealed by time-lapse fluorescence microscopy (Fig. 8A and supplementary material Movie 1) provide some of the first insight into the dynamics of peroxisome division under physiological conditions, in which a functional role of endogenous Pex11pβ was clearly delineated. We propose the following model of peroxisome division (Fig. 10): First, peroxisome division is initiated by incorporation of DHA into phospholipids in the peroxisomal membrane; second, Pex11pβ forms hyper-oligomers, and Pex11pβ-enriched regions on peroxisomal membranes are formed, initiating elongation; third, peroxisomes elongate in one direction; fourth, existing or newly-recruited DLP1 is activated on the elongated peroxisome, giving rise to peroxisome fission; and finally daughter peroxisomes bud and translocate to other regions of the cell via microtubules. DHA-induced peroxisomal division provides a model experimental system in which peroxisome division can be readily separated into distinct steps of elongation and fission under physiological conditions. This system opens new paths by which to fully elucidate the mechanisms of peroxisome morphogenesis.

Materials and Methods

Cell culture and fatty acid supplementation

Human skin fibroblasts from a normal control subject (Tig120) were purchased from the Human Science Research Resources Bank (Osaka, Japan). Fibroblasts from a patient with *AOx* deficiency (PDL30092) were previously described (Ferdinandusse et al., 2007; Poll-The et al., 1988). Fibroblasts from patients with *D-BP* deficiency (PDL20008) and X-ALD (PDL6886) were also used. All three cell lines exhibited a morphological phenotype similar to that previously described (Chang et al., 1999; Funato et al., 2006). The fibroblast cell lines, *PEX10*- (Okumoto et al., 1998a) and *PEX2*-defective cell lines (Shimozawa et al., 1992a), and MEFs were cultured at 37℃ in Dulbecco's modified Eagle's medium (DMEM; Gibco, Rockville, MD) supplemented with 10% fetal calf serum (FCS; Sigma, St Louis, MO) under 5% CO_2 (Okumoto et al., 1998b). DHA (Nacalai Tesque, Kyoto, Japan) dissolved in 4% fatty acid-free bovine serum albumin (Nacalai Tesque) in DMEM was used to supplement the cell cultures at a final concentration of 50 or 150 μM. EPA (Nacalai Tesque), α-LA (Sigma), AA (Nacalai Tesque), OA (Nacalai Tesque) and stearic acid (Sigma) were also used to supplement the cell cultures, as indicated, at a final concentration of 50 μM.

Agents and antibodies

Dynasore, nocodazole and Wy-14, 643 were purchased from Sigma. The antibodies used were rabbit antisera to rat Pex14p (Shimizu et al., 1999) and human PMP70 (Tsukamoto et al., 1990; Honsho et al., 1998), and guinea pig antisera to rat Pex14p (Mukai et al., 2002). Rabbit anti-MBP antibody was purchased from New England Biolab (Ipswich, MA). Monoclonal antibodies to human DLP1, human Tom20 (F-10), human catalase, chicken α-tubulin, and actin were purchased from BD Biosciences (Franklin Lakes, NJ), Santa Cruz Biotechnology (Santa Cruz, CA), AbFrontier (Seoul, Korea), Seikagaku Kogyo (Tokyo, Japan), and Chemicon (Temecula, CA), respectively. Rabbit antiserum against human Pex11pβ was raised as follows. An expression vector encoding the primary sequence (residues 1–203) of human (*Hs*) Pex11pβ fused to His_6, termed HsPex11pβ(1–203)-His_6, was constructed as previously described (Shimizu et al., 1999) using *Myc-HsPEX11β* (Kobayashi et al., 2007) as a template and the primers HsPEX11β(1-203)-His_6-Fw (5′-GAGGGATCCATGGACGCCTGGGTCCGC-3′) and HsPEX11β(1-203) His_6-Rv (5′-GATGAATTCATGGTGATGGTGATGAT-GACCTCTAAGGACTCGAGC-3′). A *Bam*HI–*Eco*RI fragment of the PCR product was ligated into the corresponding sites of pCold-1 (Takara). *Escherichia coli* BL21 was transformed with pCold-1-*HsPEX11β-(1-203)-*His_6 and grown according to the manufacturer's instructions. HsPex11pβ(1-203)-His_6 was solubilized from the insoluble fraction of *E. coli* lysate with 6 M guanidine hydrochloride and then recovered by Ni-NTA column chromatography (QIAGEN, Valencia, CA). The rabbit anti-Pex11pβ antibody was raised by conventional subcutaneous injection of HsPex11pβ-(1-203)-His_6 in PBS containing 0.1% Triton X-100 (Okumoto et al., 1998b). Affinity purification of the anti-Pex11pβ antibody was performed as described (Mukai et al., 2002).

RNA interference

For RNAi, ten sets of complementary antisense oligonucleotides were designed (Invitrogen, Carlsbad, CA). The sequences are listed in supplementary material Table S1. Fibroblasts were transfected twice with dsRNA at a concentration of 40 nM, with a 24-hour interval between transfections, using Lipofectamine 2000 (Invitrogen).

Morphological analysis

Cells were fixed with 4% paraformaldehyde, pH 7.4, for 15 minutes at room temperature. Peroxisomes were visualized by indirect immunofluorescence staining with the indicated antibodies, as described (Mukai et al., 2002). Antigen–antibody complexes were detected with goat anti-mouse and anti-rabbit IgG conjugated to Alexa Fluor 488 or Alexa Fluor 568 (Molecular Probes, Eugene, OR). Cells were observed under a fluorescence light microscope (Axioplan2) and by confocal laser microscopy (LSM510; Carl Zeiss, Oberkochen, Germany).

The number of peroxisomes per cell was determined for at least 50 randomly selected cells (Kim et al., 2006). Optical images obtained by confocal fluorescence microscopy were converted into threshold images and peroxisome number was calculated using the Particle Analysis package of ImageJ. Values are means ± s.d. of three independent experiments.

For time-lapse imaging analysis, *AOx*-deficient fibroblasts in 3.5-cm glass-bottom dishes were transfected with an expression vector for *HA_2-EGFP-AKL* by lipofection (Mukai and Fujiki, 2006; Okumoto et al., 1998b) and then cultured for 4 hours, followed by culture for 20 hours in the presence of 150 μM DHA. EGFP-labeled peroxisomes were monitored at 0.8-second intervals under an LSM710 microscope (Carl Zeiss, Oberkochen, Germany) equipped with an incubator and full environmental chamber (37℃ and under 5% CO_2) to maintain cell viability.

Fatty acid β-oxidation activity

Fatty acid β-oxidation activity was determined as previously described (Suzuki et al., 1991). Fibroblasts were cultured for 1 hour in DMEM in the absence of FCS. Then, 4 nmol of [^{14}C]lignoceric acid dissolved in 0.1 M Tris-HCl, pH 8.0 containing 10 mM α-cyclodextrin was added to the culture medium and cells were cultured for 2 hours. The radioactivity of acid-soluble metabolites (i.e. soluble in acetate and citrate) was counted using an LS 6500 scintillation counter (Beckman Instruments, Fullerton, CA).

Detection of mRNA by reverse transcriptase (RT)-PCR

Total RNA was extracted from cells using a FastPure RNA Kit (Takara, Kyoto, Japan) according to the manufacturer's instructions. Quantitative RT-PCR was performed using several sets of specific primers: *PEX11α* sense 5′-ACCGA-CTCTTCAGAGCCACTCAGT-3′ and antisense 5′-TCTTTGTTGATGCCAG-AGGTGAGA-3′; *PEX11β* sense 5′-CAATGTCCTGTGGGCTGGAAAGTC-3′ and antisense 5′-AGGAGCAGGACTTGCAGCCGAAGT-3′; *PPARα* sense 5′-CTGTCGGGGATGTCACACAAC-3′ and antisense 5′-GGACGATCTCCAC-AGCAAAT-3′; *ACTIN* sense 5′-TCGACAACGGCTCCGGCA-3′ and antisense 5′-AGGATCTTCATCAGGTAG-3′.

LC-MS/MS analysis

Total lipid was extracted from fibroblasts using the Bligh–Dyer method (Bligh and Dyer, 1959). Liquid chromatography–electrospray ionization coupled with tandem mass spectrometry (LC-ESI-MS/MS) was performed using a 4000 Q-TRAP quadrupole linear ion trap hybrid mass spectrometer (Applied Biosystems, MDS Sciex, Foster City, CA) with a Shimadzu Prominence HPLC System (Shimadzu, Kyoto, Japan). Samples were injected to an X Bridge C18 column (1.0 × 150 mm; Waters, Milford, MA) and then directly subjected to ESI-MS/MS analysis. A 10-μl sample volume was directly introduced by autosampler injector and the samples were separated by step gradient elution with mobile phase A (acetonitrile:methanol:water at 2:2:1 v/v/v, 0.1% formic acid and 0.028% ammonium) and mobile phase B (isopropanol, 0.1% formic acid and 0.028% ammonium) at the following ratios: 100:0 (for 0–5 minutes), 95:5 (5–20 minutes), 70:30 (20–21 minutes), 50:50 (21–45 minutes), 50:50 (45–100 min) and 100:0 (90–120 minutes). The flow rate was 70 μl/minute at 30℃. MS/MS analysis was performed in negative ion mode. Phospholipids containing DHA, EPA and AA were detected by precursor ion scanning for *m/z* 327, 301 and 303, respectively. Ion spray voltage was set at 4,500 V and collision energy was at −30 eV.

Crosslinking and sedimentation analysis

Control, *PEX10*-defective and *AOx*-deficient fibroblasts were cultured for 20 hours in the absence or presence of 150 μM DHA, EPA, or α-LA. Cells were treated for 30 minutes at room temperature with 1 mM dithiobis[succinimidyl propionate] (DSP; Pierce, Rockford, IL). After quenching with 50 mM Tris-HCl pH 7.4, for 30 minutes at room temperature, cells were harvested and solubilized with 1% Triton X-100 in 20 mM Tris-HCl, pH 7.4, 0.1 M NaCl, 1 mM EDTA, and protease inhibitor cocktail (Peptide Institute, Osaka, Japan) for 30 minutes on ice. Cell lysates were applied to the top of a continuous 5–40% sucrose density gradient in the same buffer and were centrifuged at 40,000 r.p.m. for 26 hours at 4℃ in a Beckman SW41Ti rotor (Beckman Instruments, Fullerton, CA). The gradient was fractionated into 12 tubes.

In vitro Pex11pβ oligomerization assay

1-palmitoyl-2-docosahexaenoyl-*sn*-glycero-3-phosphocholine (PDPC), 1-palmitoyl-2-oleoyl-*sn*-glycero-3-phosphocholine (POPC), 1-palmitoyl-2-docosahexaenoyl-*sn*-glycero-3-phosphoethanolamine (PDPE), and 1-palmitoyl-2-oleoyl-*sn*-glycero-3-phosphoethanolamine (POPE) were purchased from Avanti Polar Lipids (Alabaster, AL). PC and PE were purchased from Wako Pure Chemical Industries (Osaka, Japan) and Sigma, respectively. All lipids were stored in chloroform under nitrogen. To construct the plasmid encoding Pex11pβ fused to MBP, a *Kpn*I-*Bam*HI fragment of *MBP* and a *Bam*HI-*Eco*RI fragment of *HsPex11β* were ligated into the *Kpn*I and *Eco*RI sites in pCold-1. *E. coli* BL21 was transformed with pCold-1-*MBP-Pex11β* and grown according to the manufacturer's instructions. MBP–Pex11pβ was solubilized in lysis buffer (20 mM HEPES–KOH pH 7.4, 150 mM NaCl and 1% *n*-octyl-β-D-glucoside) and then recovered with amylose resin (New England Biolab). Recombinant MBP–Pex11pβ was eluted with elution buffer (20 mM HEPES–KOH pH 7.4, 150 mM NaCl, 0.1% *n*-octyl-β-D-glucoside and 10 mM maltose), according to the manufacturer's procedure.

For the preparation of SL (60% PC and 40% PE), DL (35% PC, 29% PE, 25% PDPC and 11% PDPE) and OL (35% PC, 29% PE, 25% POPC and 11% POPE), the appropriate amounts (w/w) of lipid were mixed, dried under nitrogen, and then rehydrated in 0.3 M sucrose. MBP–Pex11pβ was then mixed with the liposomes. Mixtures were frozen once at −80℃ and then diluted in 20 mM HEPES–KOH pH 7.4 containing 150 mM NaCl. Proteoliposomes were solubilized with 1% Triton X-100, applied onto the top of a continuous 1–30% glycerol density-gradient, and then centrifuged at 30,000 r.p.m. for 18 hours at 4℃ in a Beckman SW41Ti rotor. After centrifugation, the gradient was fractionated into ten tubes.

Acknowledgements

We thank M. Nishi for preparing figures and the other members of our laboratory for discussion.

Funding

This work was supported in part by CREST grant (to Y.F.) from the Science and Technology Agency of Japan; Grants-in-Aid for Scientific Research (to Y.F.), and The Global COE Program from The Ministry of Education, Culture, Sports, Science, and Technology of Japan; grants (to Y.F.) from Takeda Science Foundation and Japan Foundation for Applied Enzymology. A.I. is supported by a Research Fellowship of CREST.

Supplementary material available online at
http://jcs.biologists.org/lookup/suppl/doi:10.1242/jcs.087452/-/DC1

References

Abe, I. and Fujiki, Y. (1998). cDNA cloning and characterization of a constitutively expressed isoform of the human peroxin Pex11p. *Biochem. Biophys. Res. Commun.* **252**, 529-533.

Abe, I., Okumoto, K., Tamura, S. and Fujiki, Y. (1998). Clofibrate-inducible, 28-kDa peroxisomal integral membrane protein is encoded by *PEX11*. *FEBS Lett.* **431**, 468-472.

Barnett, P., Tabak, H. F. and Hettema, E. H. (2000). Nuclear receptors arose from pre-existing protein modules during evolution. *Trends Biochem. Sci.* **25**, 227-228.

Bligh, E. G. and Dyer, W. J. (1959). A rapid method of total lipid extraction and purification. *Can. J. Med. Sci.* **37**, 911-917.

Chang, C. C., South, S., Warren, D., Jones, J., Moser, A. B., Moser, H. W. and Gould, S. J. (1999). Metabolic control of peroxisome abundance. *J. Cell Sci.* **112**, 1579-1590.

Crane, D. I. and Masters, C. J. (1986). The effect of clofibrate on the phospholipid composition of the peroxisomal membranes in mouse liver. *Biochim. Biophys. Acta.* **876**, 256-263.

Delille, H. K., Agricola, B., Guimaraes, S. C., Borta, H., Lüers, G. H., Fransen, M. and Schrader, M. (2010). Pex11pβ-mediated growth and division of mammalian peroxisomes follows a maturation pathway. *J. Cell Sci.* **123**, 2750-2762.

Ferdinandusse, S., Denis, S., Mooijer, P. A., Zhang, Z., Reddy, J. K., Spector, A. A. and Wanders, R. J. (2001). Identification of the peroxisomal β-oxidation enzymes involved in the biosynthesis of docosahexaenoic acid. *J. Lipid Res.* **42**, 1987-1995.

Ferdinandusse, S., Denis, S., Mooijer, P. A., Dekker, C., Duran, M., Soorani-Lunsing, R. J., Boltshauser, E., Macaya, A., Gärtner, J., Majoie, C. B. et al. (2006). Clinical and biochemical spectrum of D-bifunctional protein deficiency. *Ann. Neurol.* **59**, 92-104.

Ferdinandusse, S., Denis, S., Hogenhout, E. M., Koster, J., van Roermund, C. W. T., IJlst, L., Moser, A. B., Wanders, R. J. A. and Waterham, H. R. (2007). Clinical, biochemical, and mutational spectrum of peroxisomal acyl-coenzyme A oxidase deficiency. *Hum. Mutat.* **28**, 904-912.

Fujiki, Y. (2000). Peroxisome biogenesis and peroxisome biogenesis disorders. *FEBS Lett.* **476**, 42-46.

Funato, M., Shimozawa, N., Nagase, T., Takemoto, Y., Suzuki, Y., Imamura, Y., Matsumoto, T., Tsukamoto, T., Kojidani, T., Osumi, T. et al. (2006). Aberrant peroxisome morphology in peroxisomal β-oxidation enzyme deficiencies. *Brain Dev.* **5**, 287-292.

Gandre-Babbe, S. and van der Bliek, A. M. (2008). The novel tail-anchored membrane protein Mff controls mitochondrial and peroxisomal fission in mammalian cells. *Mol. Biol. Cell* **19**, 2402-2412.

Gondcaille, C., Depreter, M., Fourcade, S., Lecca, M. R., Leclercq, S., Martin, P. G., Pineau, T., Cadepond, F., ElEtr, M., Bertrand, N. et al. (2005). Phenylbutyrate up-regulates the adrenoleukodystrophy-related gene as a nonclassical peroxisome proliferator. *J. Cell Biol.* **169**, 93-104.

Gould, S. J. and Valle, D. (2000). Peroxisome biogenesis disorders: genetics and cell biology. *Trends in Genetics* **16**, 340-345.

Guo, T., Gregg, C., Boukh-Viner, T., Kyryakov, P., Goldberg, A., Bourque, S., Banu, F., Haile, S., Milijevic, S., San, K. H. et al. (2007). A signal from inside the peroxisome initiates its division by promoting the remodeling of the peroxisomal membrane. *J. Cell Biol.* **177**, 289-303.

Honsho, M., Tamura, S., Shimozawa, N., Suzuki, Y., Kondo, N. and Fujiki, Y. (1998). Mutation in *PEX16* is causal in the peroxisome-deficient Zellweger syndrome of complementation group D. *Am. J. Hum. Genet.* **63**, 1622-1630.

Ingerman, E., Perkins, E. M., Marino, M., Mears, J. A., McCaffery, J. M., Hinshaw, J. E. and Nunnari, J. (2005). Dnm1 forms spirals that are structurally tailored to fit mitochondria. *J. Cell Biol.* **170**, 1021-1027.

Kemp, S., Wei, H.-M., Lu, J.-F., Braiterman, L. T., McGuinness, M. C., Moser, A. B., Watkins, P. A. and Smith, K. D. (1998). Gene redundancy and pharmacological gene therapy: implications for X-linked adrenoleukodystrophy. *Nat. Med.* **4**, 1261-1268.

Kemp, S., Pujol, A., Waterham, H. R., van Geel, B. M., Boehm, C. D., Raymond, G. V., Cutting, G. R., Wanders, R. J. and Moser, H. W. (2001). ABCD1 mutations and the X-linked adrenoleukodystrophy mutation database: role in diagnosis and clinical correlations. *Hum. Mutat.* **18**, 499-515.

Kim, P. K., Mullen, R. T., Schumann, U. and Lippincott-Schwartz, J. (2006). The origin and maintenance of mammalian peroxisomes involves a de novo PEX16-dependent pathway from the ER. *J. Cell Biol.* **173**, 521-532.

Kobayashi, S., Tanaka, A. and Fujiki, Y. (2007). Fis1, DLP1, and Pex11p coordinately regulate peroxisome morphogenesis. *Exp. Cell Res.* **313**, 1675-1686.

Koch, A., Thiemann, M., Grabenbauer, M., Yoon, Y., McNiven, M. A. and Schrader, M. (2003). Dynamin-like protein 1 is involved in peroxisomal fission. *J. Biol. Chem.* **278**, 8597-8605.

Koch, A., Schneider, G., Lüers, G. H. and Schrader, M. (2004). Peroxisome elongation and constriction but not fission can occur independently of dynamin-like protein 1. *J. Cell Sci.* **117**, 3995-4006.

Koch, A., Yoon, Y., Bonekamp, N. A., McNiven, M. A. and Schrader, M. (2005). A role for Fis1 in both mitochondrial and peroxisomal fission in mammalian cells. *Mol. Biol. Cell* **16**, 5077-5086.

Koch, J., Pranjic, K., Huber, A., Ellinger, A., Hartig, A., Kragler, F. and Brocard, C. (2010). PEX11 family members are membrane elongation factors that coordinate peroxisome proliferation and maintenance. *J. Cell Sci.* **123**, 3389-3400.

Krey, G., Braissant, O., L'Horset, F., Kalkhoven, E., Perroud, M., Parker, M. G. and Wahli, W. (1997). Fatty acids, eicosanoids, and hypolipidemic agents identified as ligands of peroxisome proliferator-activated receptors by coactivator-dependent receptor ligand assay. *Mol. Endocrinol.* **11**, 779-791.

Lazarow, P. B. and Fujiki, Y. (1985). Biogenesis of peroxisomes. *Ann. Rev. Cell Biol.* **1**, 489-530.

Li, X. and Gould, S. J. (2002). PEX11 promotes peroxisome division independently of peroxisome metabolism. *J. Cell Biol.* **156**, 643-651.

Li, X. and Gould, S. J. (2003). The dynamin-like GTPase DLP1 is essential for peroxisome division and is recruited to peroxisomes in part by PEX11. *J. Biol. Chem.* **278**, 17012-17020.

Li, X., Baumgart, E., Dong, G. X., Morrell, J. C., Jimenez-Sanchez, G., Valle, D., Smith, K. D. and Gould, S. J. (2002a). PEX11 is required for peroxisome proliferation in response to 4-phenylbutyrate but is dispensable for peroxisome proliferator-activated receptor alpha-mediated peroxisome proliferation. *Mol. Cell. Biol.* **22**, 8226-8240.

Li, X., Baumgart, E., Morrell, J. C., Jimenez-Sanchez, G., Valle, D. and Gould, S. J. (2002b). PEX11β deficiency is lethal and impairs neuronal migration but does not abrogate peroxisome function. *Mol. Cell. Biol.* **22**, 4358-4365.

Macia, E., Ehrlich, M., Massol, R., Boucrot, E., Brunner, C. and Kirchhausen, T. (2006). Dynasore, a cell-permeable inhibitor of dynamin. *Dev. Cell* **10**, 839-850.

Marshall, P. A., Dyer, J. M., Quick, M. E. and Goodman, J. M. (1996). Redox-sensitive homodimerization of Pex11p: a proposed mechanism to regulate peroxisomal division. *J. Cell Biol.* **135**, 123-137.

Martinez, M. (1995). Polyunsaturated fatty acids in the developing human brain, erythrocytes and plasma in peroxisomal disease: therapeutic implications. *J. Inherit. Metab. Dis.* **18 Suppl. 1**, 61-75.

Mosser, J., Douar, A.-M., Sarde, C.-O., Kioschis, P. R. F., Moser, H., Poustka, A.-M., Mandel, J.-L. and Aubourg, P. (1993). Putative X-linked adrenoleukodystrophy gene shares unexpected homology with ABC transporters. *Nature* **361**, 726-730.

Mukai, S. and Fujiki, Y. (2006). Molecular mechanisms of import of peroxisome-targeting signal type 2 (PTS2) proteins by PTS2 receptor Pex7p and PTS1 receptor Pex5pL. *J. Biol. Chem.* **281**, 37311-37320.

Mukai, S., Ghaedi, K. and Fujiki, Y. (2002). Intracellular localization, function, and dysfunction of the peroxisome-targeting signal type 2 receptor, Pex7p, in mammalian cells. *J. Biol. Chem.* **277**, 9548-9561.

Okumoto, K., Itoh, R., Shimozawa, N., Suzuki, Y., Tamura, S., Kondo, N. and Fujiki, Y. (1998a). Mutation in *PEX10* is the cause of Zellweger peroxisome deficiency syndrome of complementation group B. *Hum. Mol. Genet.* **7**, 1399-1405.

Okumoto, K., Shimozawa, N., Kawai, A., Tamura, S., Tsukamoto, T., Osumi, T., Moser, H., Wanders, R. J. A., Suzuki, Y., Kondo, N. et al. (1998b). *PEX12*, the pathogenic gene of group III Zellweger syndrome: cDNA cloning by functional complementation on a CHO cell mutant, patient analysis, and characterization of Pex12p. *Mol. Cell. Biol.* **18**, 4324-4336.

Pitts, K. R., Yoon, Y., Krueger, E. W. and McNiven, M. A. (1999). The dynamin-like protein DLP1 is essential for normal distribution and morphology of the endoplasmic reticulum and mitochondria in mammalian cells. *Mol. Biol. Cell* **10**, 4403-4417.

Poll-The, B. T., Roels, E., Ogier, H., Scotto, J., Vamecq, J., Schutgens, R. B. H., van Roermund, C. W. T., van Wijland, M. J. A., Schram, A. W., Tager, J. M. et al. (1988). A new peroxisomal disorder with enlarged peroxisomes and a specific deficiency of acyl-CoA oxidase (pseudo-neonatal adrenoleukodystrophy). *Am. J. Hum. Genet.* **42**, 422-434.

Santos, M. J., Imanaka, T., Shio, H., Small, G. M. and Lazarow, P. B. (1988). Peroxisomal membrane ghosts in Zellweger syndrome- aberrant organelle assembly. *Science* **239**, 1536-1538.

Schollenberger, L., Gronemeyer, T., Huber, C. M., Lay, D., Wiese, S., Meyer, H. E., Warscheid, B., Saffrich, R., Peränen, J., Gorgas, K. et al. (2010). RhoA regulates peroxisome association to microtubules and the actin cytoskeleton. *PLoS ONE* **5**, e13886.

Schrader, M., Reuber, B. E., Morrell, J. C., Jimenez-Sanchez, G., Obie, C., Stroh, T. A., Valle, D., Schroer, T. A. and Gould, S. J. (1998). Expression of *PEX11β* mediates peroxisome proliferation in the absence of extracellular stimuli. *J. Biol. Chem.* **273**, 29607-29614.

Shimizu, N., Itoh, R., Hirono, Y., Otera, H., Ghaedi, K., Tateishi, K., Tamura, S., Okumoto, K., Harano, T., Mukai, S. et al. (1999). The peroxin Pex14p: cDNA cloning by functional complementation on a Chinese hamster ovary cell mutant, characterization, and functional analysis. *J. Biol. Chem.* **274**, 12593-12604.

Shimizu, M., Takeshita, A., Tsukamoto, T., Gonzalez, F. J. and Osumi, T. (2004). Tissue-selective, bidirectional regulation of PEX11α and perilipin genes through a common peroxisome proliferator response element. *Mol. Cell. Biol.* **24**, 1313-1323.

Shimizu, T., Ohto, T. and Kita, Y. (2006). Cytosolic phospholipase A2: biochemical properties and physiological roles. *IUBMB Life* **58**, 328-333.

Shimozawa, N., Tsukamoto, T., Suzuki, Y., Orii, T. and Fujiki, Y. (1992a). Animal cell mutants represent two complementation groups of peroxisome-defective Zellweger syndrome. *J. Clin. Invest.* **90**, 1864-1870.

Shimozawa, N., Tsukamoto, T., Suzuki, Y., Orii, T., Shirayoshi, Y., Mori, T. and Fujiki, Y. (1992b). A human gene responsible for Zellweger syndrome that affects peroxisome assembly. *Science* **255**, 1132-1134.

Shindou, H. and Shimizu, T. (2009). Acyl-CoA:lysophospholipid acyltransferases. *J. Biol. Chem.* **284**, 1-5.

Smith, K. D., Kemp, S., Braiterman, L. T., Lu, J. F., Wei, H. M., Geraghty, M., Stetten, G., Bergin, J. S., Pevsner, J. and Watkins, P. A. (1999). X-linked adrenoleukodystrophy: genes, mutations, and phenotypes. *Neurochem. Res.* **24**, 521-535.

Su, H. M., Moser, A. B., Moser, H. W. and Watkins, P. A. (2001). Peroxisomal straight-chain Acyl-CoA oxidase and D-bifunctional protein are essential for the retroconversion step in docosahexaenoic acid synthesis. *J. Biol. Chem.* **276**, 38115-38120.

Subramani, S. (1998). Components involved in peroxisome import, biogenesis, proliferation, turnover, and movement. *Physiol. Rev.* **78**, 171-188.

Suzuki, Y., Shimozawa, N., Yajima, S., Yamaguchi, S., Orii, T. and Hashimoto, T. (1991). Effects of sodium 2-[5-(4-chlorophenyl)pentyl]-oxirane-2-carboxylate (POCA) on fatty acid oxidation in fibroblasts from patients with peroxisomal diseases. *Biochem. Pharmacol.* **41**, 453-456.

Suzuki, Y., Jiang, L. L., Souri, M., Miyazawa, S., Fukuda, S., Zhang, Z., Une, M., Shimozawa, N., Kondo, N., Orii, T. and Hashimoto, T. (1997). D-3-hydroxyacyl-CoA dehydratase/D-3-hydroxyacyl-CoA dehydrogenase bifunctional protein deficiency: a newly identified peroxisomal disorder. *Am. J. Hum. Genet.* **61**, 1153-1162.

Tanaka, A., Okumoto, K. and Fujiki, Y. (2003). cDNA cloning and characterization of the third isoform of human peroxin Pex11p. *Biochem. Biophys. Res. Commun.* **300**, 819-823.

Tanaka, A., Kobayashi, S. and Fujiki, Y. (2006). Peroxisome division is impaired in a CHO cell mutant with an inactivating point-mutation in dynamin-like protein 1 gene. *Exp. Cell Res.* **312**, 1671-1684.

Tsukamoto, T., Yokota, S. and Fujiki, Y. (1990). Isolation and characterization of Chinese hamster ovary cell mutants defective in assembly of peroxisomes. *J. Cell Biol.* **110**, 651-660.

Wanders, R. J. (2004). Peroxisomes, lipid metabolism, and peroxisomal disorders. *Mol. Genet. Metab.* **83**, 16-27.

Wanders, R. J. and Waterham, H. R. (2006). Peroxisomal disorders: the single peroxisomal enzyme deficiencies. *Biochim. Biophys. Acta* **1763**, 1707-1720.

Warren, D. S., Morrell, J. C., Moser, H. W., Valle, D. and Gould, S. J. (1998). Identification of *PEX10*, the gene defective in complementation group 7 of the peroxisome-biogenesis disorders. *Am. J. Hum. Genet.* **63**, 347-359.

Waterham, H. R., Koster, J., van Roermund, C. W. T., Mooyer, P. A. W., Wanders, R. J. A. and Leonard, J. V. (2007). A lethal defect of mitochondrial and peroxisomal fission. *N. Engl. J. Med.* **356**, 1736-1741.

Wei, H., Kemp, S., McGuinness, M. C., Moser, A. B. and Smith, K. D. (2000). Pharmacological induction of peroxisomes in peroxisome biogenesis disorders. *Ann. Neurol.* **47**, 286-296.

Wiemer, E. A. C., Wenzel, T., Deerinck, T. J., Ellisman, M. H. and Subramani, S. (1997). Visualization of the peroxisomal compartment in living mammalian cells: dynamic behavior and association with microtubules. *J. Cell Biol.* **136**, 71-80.

Yang, J., Han, X. and Gross, R. W. (2003). Identification of hepatic peroxisomal phospholipase A(2) and characterization of arachidonic acid-containing choline glycerophospholipids in hepatic peroxisomes. *FEBS Lett.* **546**, 247-250.

Yoon, Y. S., Yoon, D. S., Lim, I. K., Yoon, S. H., Chung, H. Y., Rojo, M., Malka, F., Jou, M. J., Martinou, J. C. and Yoon, G. (2006). Formation of elongated giant mitochondria in DFO-induced cellular senescence: involvement of enhanced fusion process through modulation of Fis1. *J. Cell Physiol.* **209**, 468-480.